

Supporting Information

Identification of Functional Substates of KRas during GTP

Hydrolysis with Enhanced Sampling Simulations

Juan Zeng,[†] Jian Chen,[‡] Fei Xia^{*,‡}, Qiang Cui,[#] Xianming Deng^{*,†} and Xin Xu^{*,¶}

[†]*School of Biomedical Engineering, Guangdong Medical University, Dongguan 523808, China*

[‡]*School of Chemistry and Molecular Engineering, NYU-ECNU Center for Computational Chemistry at NYU Shanghai, East China Normal University, Shanghai 200062, China*

[#]*Departments of Chemistry, Physics and Biomedical Engineering, Boston University, 590 Commonwealth Avenue, Boston, MA 02215, United States*

[†]*State Key Laboratory of Cellular Stress Biology Innovation Center for Cell Signaling Network, School of Life Sciences, Xiamen University, Fujian 361101, China*

[¶]*Collaborative Innovation Center of Chemistry for Energy Materials, Shanghai Key Laboratory of Molecular Catalysis and Innovative Materials, MOE Key Laboratory of Computational Physical Sciences, Departments of Chemistry, Fudan University, Shanghai 200433, China*

Table S1. Summary of the PDB IDs for the experimental structures used in this work.

Figure S1 Distance restraints applied to the hydrogen-bonding network at the active sites of HRasGTP·Mg²⁺ and HRasGDP·Mg²⁺.

Figure S2 The calculated exchange ratios, the RMSD and Rg values of every 50 ns and the distributions of helix and RMSD at different temperatures.

Figure S3 Comparison for the orientations of Tyr32 in the crystal structures of Raf·KRas and Raf·HRas.

Figure S4 Comparison for the orientations of Tyr32 in the crystal structures of GAP·HRas and HRas.

Figure S5 Comparison for the conformations of the Arg finger in the crystal structures of complexes GAP·HRas and GAP·KRas.

Figure S6 H-bond networks at the active sites of KRasGTP·Mg²⁺_{s2} and KRasGDP·Pi·Mg²⁺_{s2}.

Figure S7 Calculated RMSD values for the heavy atoms in three KRas complex systems: KRas^{GEF}, KRas^{GEF}GDP·Mg²⁺ and KRas^{GEF}GTP·Mg²⁺.

Figure S8 Overlapped representative structures of conformations of KRas^{GEF}_{s1}, KRas^{GEF}GDP·Mg²⁺_{s1} and KRas^{GEF}GTP·Mg²⁺.

Figure S9 Calculated RMSD values of the heavy atoms of the high-energy structures.

Table S1. Summary of the PDB IDs for the experimental structures used in this work.

PDB ID	State
3GFT	S2
4OBE	S1
5W22	S1
6MBT	S1
6MBU	S1
6EPL	GEF·KRas
6OB2	GAP·KRas
6OB3	GAP·KRas_{G13D}
1WQ1	GAP·HRas
2MSE	Raf·KRas
4G0N	Raf·HRas

Figure S1. Distance restraints applied to the hydrogen-bonding network at the active sites of HRasGTP·Mg²⁺ and HRasGDP·Mg²⁺. (a) The dashed lines denote the six distance restraints (with equilibrium values based on the corresponding crystal structure and a force constant of 500 kcal/mol/Å²) applied to the Mg²⁺ ion, the oxygen atoms of GTP, D57, S17 and the water molecule at the active site of KRasGTP·Mg²⁺. (b) The dashed lines denote the five distance restraints applied to the Mg²⁺ ion, the oxygen atom of GTP, D57, S17 and the water molecule at the active site of KRasGDP·Mg²⁺. The restraints applied in the KRasGDP·Pi·Mg²⁺ system are similar to those in KRasGDP·Mg²⁺.

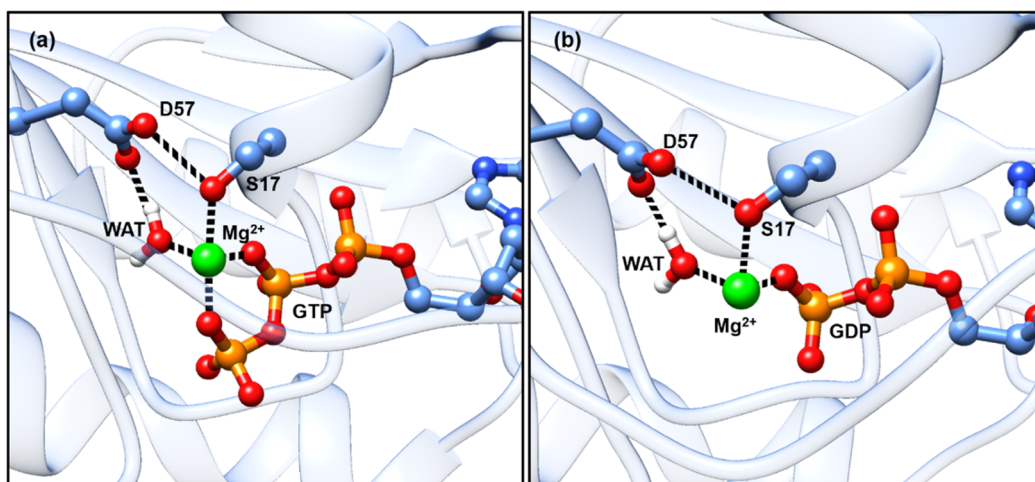


Figure S2 The calculated exchange ratios, the RMSD and Rg values of every 50 ns and the distributions of helix and RMSD at different temperatures. (a) The calculated fraction exchange ratios from the REMD simulations of the KRasGTP·Mg²⁺_{3GFT}, KRasGTP·Mg²⁺_{4OBE}, KRasGDP·Pi·Mg²⁺ and KRasGDP·Mg²⁺ are in the moderate range of 0.3-0.5, where the subscripts of the first two structures denote their initial structures. (b) The calculated RMSD and Rg values of every 50 ns of KRasGTP·Mg²⁺_{3GFT} indicates the convergence of the 100-350 ns REMD trajectory. (c) In the left plot, the calculated probability of helix of the KRasGTP·Mg²⁺_{3GFT} systems at different temperatures indicates that no unfolding of helices take place. The right plot shows the distribution of the calculated RMSD values of all heavy atoms at each temperature; as expected, the RMSD values generally increase as the temperature increases.

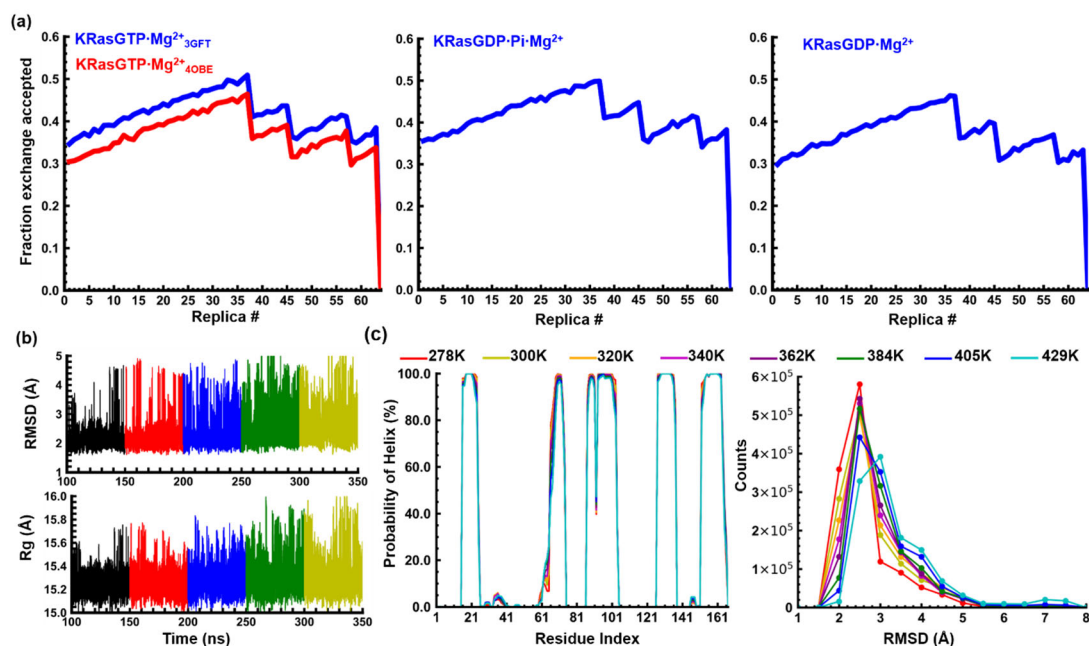


Figure S3 Comparison for the orientations of Tyr32 in the crystal structures of Raf·KRas and Raf·HRas. Tyr32 in both complexes adopts the “Tyr32_{in}” conformation.

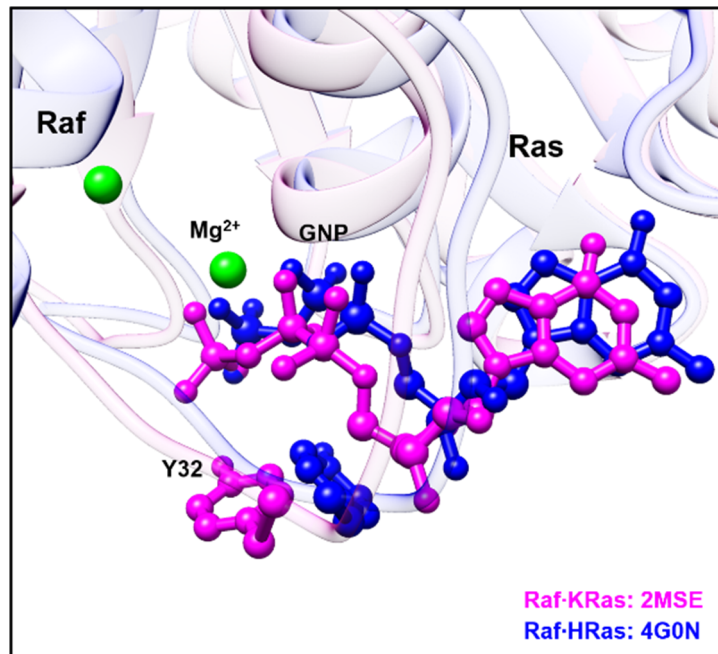


Figure S4 Comparison for the orientations of Tyr32 in the crystal structures of GAP·HRas and HRas. In the complex GAP·HRas, the Arg finger (R789) remains in the proximity of the substrate, while Tyr32 is oriented in the “Tyr32_{out}” conformation. Tyr32 in 1QRA is also oriented in the “Tyr32_{out}” conformation similar to the situation in GAP·HRas.

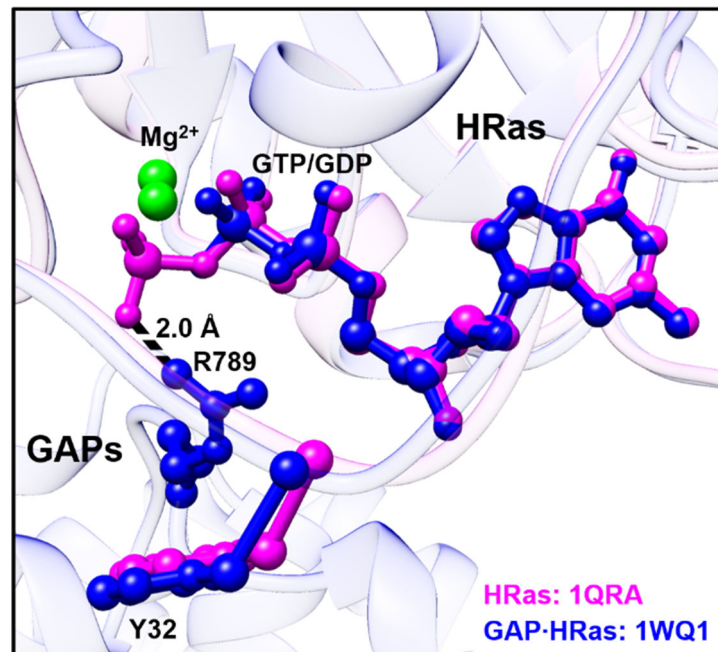


Figure S5 Comparison for the conformations of the Arg finger in the crystal structures of GAP·HRas and GAP·KRas. The Arg finger (R789) in GAP·HRas is close to the substate, while Tyr32 adopts the “Tyr32_{out}” conformation. By contrast, the Arg finger (R1276) in GAP·KRas remains far from the substate, although Tyr32 also adopts the “Tyr32_{out}” orientation.

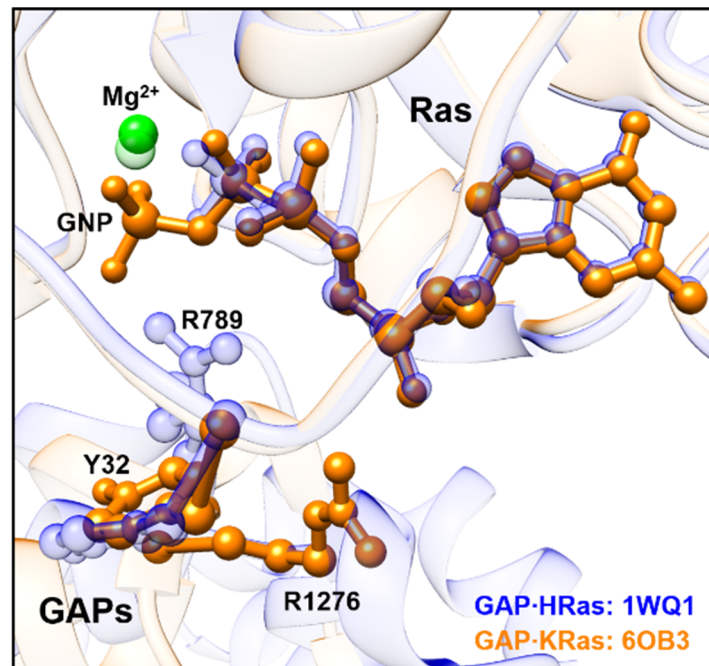


Figure S6 H-bond networks at the active sites of KRasGTP·Mg²⁺_{s2} and KRasGDP·Pi·Mg²⁺_{s2}. (a) The H-bond network at the active site of KRasGTP·Mg²⁺_{s2}, where the dashed lines denote the pairwise interactions of the Mg²⁺ ion, the oxygen atoms of GTP, D57, S17, T35 and the water molecules. (b) The H-bond network at the active site of KRasGDP·Pi·Mg²⁺_{s2}, where the dashed lines denote the pairwise interactions to the Mg²⁺ ion, the oxygen atoms of GTP, Pi, D57, S17, T35 and the water molecules.

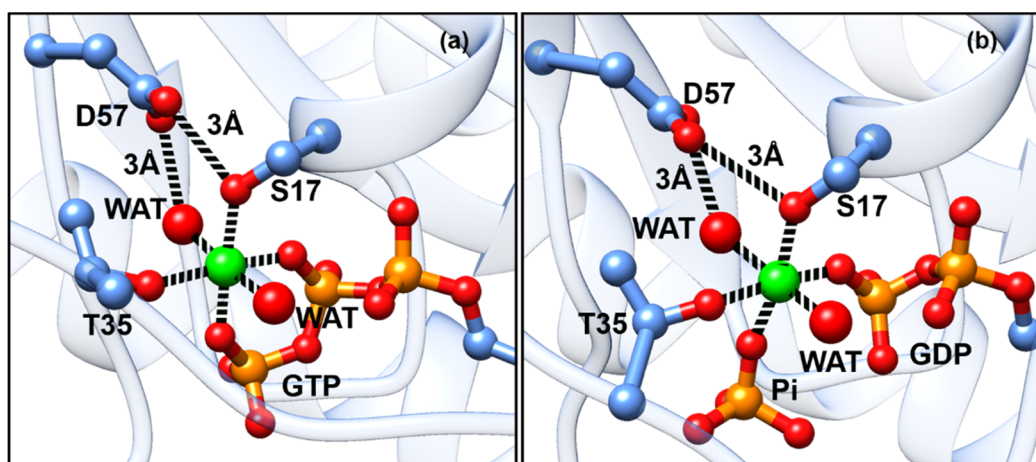


Figure S7 Calculated RMSD values (relative to 3GFT) for heavy atoms in the three KRas complex systems: KRas^{GEF}, KRas^{GEF}GDP·Mg²⁺ and KRas^{GEF}GTP·Mg²⁺ in 500 ns unbiased MD trajectories.

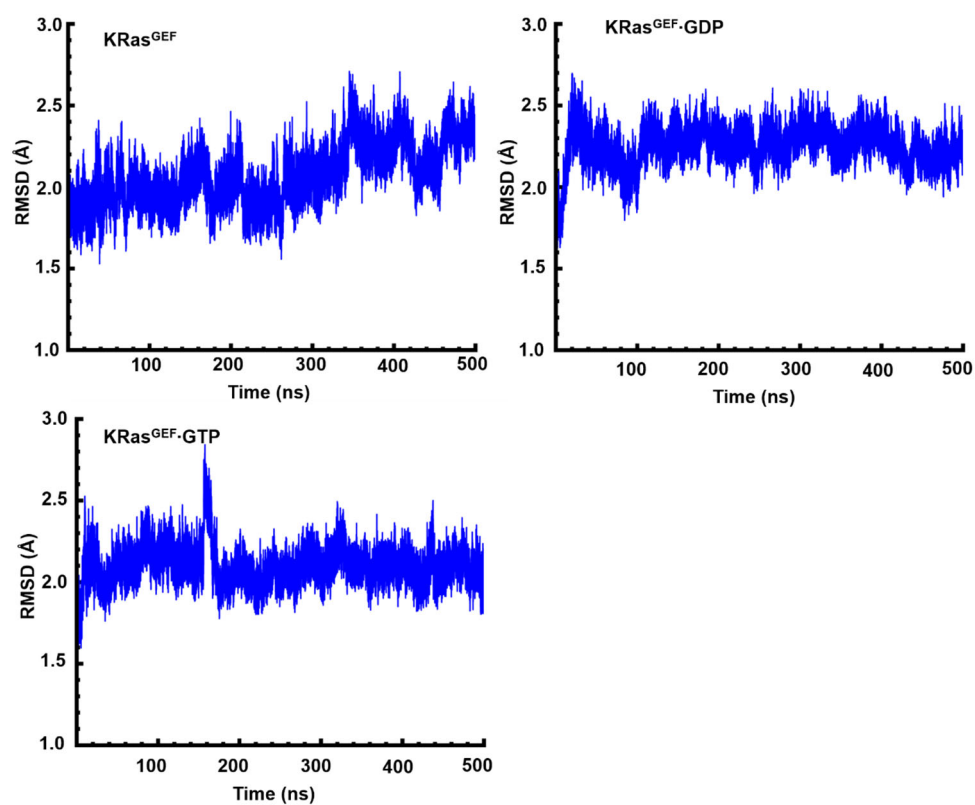


Figure S8 Overlapped representative structures of KRas^{GEF}_{S1}, KRas^{GEF}GDP·Mg²⁺_{S1} and KRas^{GEF}GTP·Mg²⁺_{S1} from 300-ns canonical simulation.

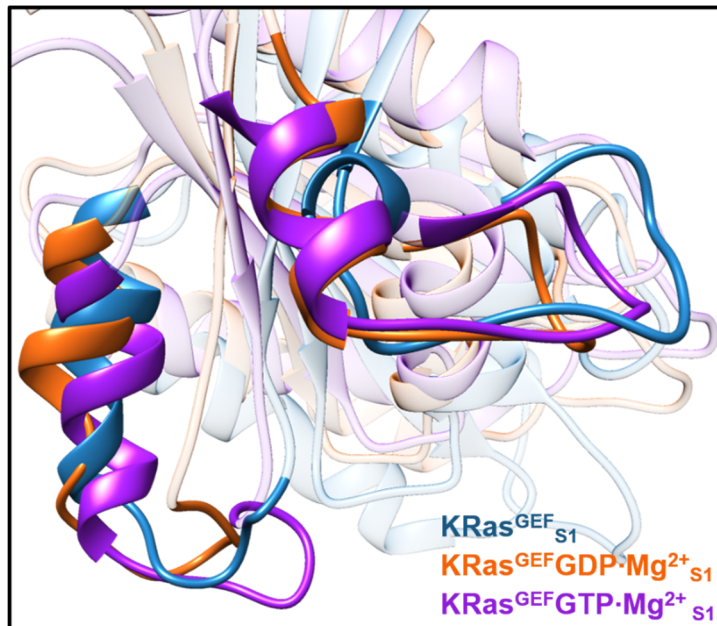


Figure S9 Calculated RMSD values of the heavy atoms of the high-energy structures. The calculated RMSD curves are relative to the reference 3GFT from the 300 ns MD simulations of KRasGTP·Mg²⁺_{S1.2}, KRasGDP·Pi·Mg²⁺_{S1.1}, KRasGDP·Pi·Mg²⁺_{S1.2} and KRasGDP·Mg²⁺_{S1.2} with the initial structures extracted from their 2D-FELs. The RMSD values of KRasGTP·Mg²⁺_{S1.2} fluctuate around 4.0 Å, higher than the 3.4 Å of KRasGTP·Mg²⁺_{S1.1} in Figure 3a. The RMSD values of KRasGDP·Pi·Mg²⁺_{S1.1} and KRasGDP·Pi·Mg²⁺_{S1.2} fluctuate around 3.2 and 4.2 Å, higher than the value of 2.0 Å of KRasGDP·Pi·Mg²⁺_{S2} in Figure 4a. The RMSD values of KRasGDP·Mg²⁺_{S1.2} fluctuate around 4.4 Å, higher than the 3.4 Å of KRasGDP·Mg²⁺_{S1.1} in Figure 6a.

